

18. Van der Voo, R. *Paleomagnetism of the Atlantic, Tethys and Iapetus Oceans* (Cambridge University Press, Cambridge, 1993).
19. De Wever, P., Azéma, J. & Fourcade, E. Radiolaires et radiolarites: production primaire, diagenèse et paléogéographie. *Bull. Centres Rech. Explor. Product. Elf Aquitaine* **18**, 315–379 (1994).
20. Baumgartner, P. O. Age and genesis of Tethyan Jurassic Radiolarites. *Eclog. Geol. Helv.* **80**, 831–879 (1987).
21. Bartolini, A., Baumgartner, P. O. & Guex, J. Middle and Late Jurassic radiolarian palaeoecology versus carbon-isotope stratigraphy. *Palaeogeogr. Palaeoclimatol. Palaeoecol.* **145**, 43–60 (1999).
22. Bernoulli, D., Manatschal, G., Desmurs, L. & Muentener, O. Where did Gustav Steinmann see the trinity? Back to the roots of an Alpine ophiolite concept. *Geol. Soc. Am. Spec. Pap.* **373**, 93–110 (2003).
23. Richards, D., Butler, R. F. & Harms, T. A. Paleomagnetism of the late Paleozoic Slide Mountain terrane, northern and central British Columbia. *Can. J. Earth Sci.* **30**, 1898–1913 (1993).
24. Hagstrum, J. T. & Murchey, B. L. Deposition of Franciscan Complex cherts along the paleoequator and accretion to the American margin at tropical paleolatitudes. *Geol. Soc. Am. Bull.* **105**, 766–778 (1993).
25. Larson, R. L., Steiner, M. B., Erba, E. & Lancelot, Y. Paleolatitudes and tectonic reconstructions of the oldest portion of the Pacific Plate: A comparative study. *Proc. ODP. Sci. Res.* **129**, 615–631 (1992).
26. Besse, J. & Courtillot, V. Correction to “Apparent and true polar wander and the geometry of the geomagnetic field over the last 200 Myr”. *J. Geophys. Res. Solid Earth* **108**, 2469, doi:10.1029/2003JB002684 (2003).
27. McFadden, P. L. & Lowes, F. J. The discrimination of mean directions drawn from Fisher distributions. *Geophys. J. R. Astron. Soc.* **67**, 19–33 (1981).
28. Lottes, A. L. & Rowley, D. B. in *Paleozoic Palaeogeography and Biogeography* (eds McKerrow, W. S. & Scotese, C. R.) 383–395 (Memoir 12, Geological Society of London, 1990).
29. Bullard, E. C., Everett, J. & Smith, A. G. The fit of the continents around the Atlantic. *Phil. Trans. R. Soc. Lond. A* **258**, 41–45 (1965).
30. Klitgord, K. D. & Schouten, H. in *The Geology of North America, The Western North Atlantic Region* (eds Vogt, P. R. & Tucholke, B. E.) 351–377 (Geological Society of America, Boulder, 1986).

**Supplementary Information** accompanies the paper on [www.nature.com/nature](http://www.nature.com/nature).

**Acknowledgements** E. Dallanave is thanked for assistance in the field and laboratory analysis. Comments by D. Bernoulli and J. Hagstrum greatly improved the manuscript.

**Competing interests statement** The authors declare that they have no competing financial interests.

**Correspondence** and requests for materials should be addressed to G.M. ([giovanni.muttoni1@unimi.it](mailto:giovanni.muttoni1@unimi.it)).

## Insolation-driven changes in atmospheric circulation over the past 116,000 years in subtropical Brazil

Francisco W. Cruz Jr<sup>1,2</sup>, Stephen J. Burns<sup>1</sup>, Ivo Karmann<sup>2</sup>, Warren D. Sharp<sup>3</sup>, Mathias Vuille<sup>1</sup>, Andrea O. Cardoso<sup>4</sup>, José A. Ferrari<sup>5</sup>, Pedro L. Silva Dias<sup>4</sup> & Oduvaldo Viana Jr<sup>2</sup>

<sup>1</sup>Department of Geosciences, University of Massachusetts, Amherst, 01002 Massachusetts, USA

<sup>2</sup>Instituto de Geociências, Universidade de São Paulo, Rua do Lago 562, São Paulo, SP, 05508-080, Brazil

<sup>3</sup>Berkeley Geochronology Center, 2455 Ridge Rd, Berkeley, California 94709, USA

<sup>4</sup>Departamento de Ciências Atmosféricas, Instituto de Astronomia, Geofísica e Ciências Atmosféricas, Universidade de São Paulo, Rua do Matão 1226, São Paulo, SP 05508-090, Brazil

<sup>5</sup>Instituto Geológico, Av. Miguel Stefano 3900, São Paulo, SP 04301-903, Brazil

During the last glacial period, large millennial-scale temperature oscillations—the ‘Dansgaard/Oeschger’ cycles—were the primary climate signal in Northern Hemisphere climate archives from the high latitudes to the tropics<sup>1–6</sup>. But whether the influence of these abrupt climate changes extended to the tropical and subtropical Southern Hemisphere, where changes in insolation are thought to be the main direct forcing of climate, has remained unclear. Here we present a high-resolution oxygen isotope record of a U/Th-dated stalagmite from subtropical southern Brazil, covering the past 116,200 years. The oxygen isotope signature varies with shifts in the source region and amount of rainfall in the area, and hence records changes in

atmospheric circulation and convective intensity over South America. We find that these variations in rainfall source and amount are primarily driven by summer solar radiation, which is controlled by the Earth’s precessional cycle. The Dansgaard/Oeschger cycles can be detected in our record and therefore we confirm that they also affect the tropical hydrological cycle, but that in southern subtropical Brazil, millennial-scale climate changes are not as dominant as they are in the Northern Hemisphere.

The study area in subtropics of southeastern Brazil is well-situated for investigating changes in tropical and subtropical atmospheric circulation. Although wet and dry seasons are not observed, the region receives rainfall from two distinct sources in different seasons (see Supplementary Information S1). During the austral winter and early spring, equatorward incursions of mid-latitude cold dry air result in cyclonic storms that move moisture inland from the nearby Atlantic Ocean<sup>7</sup>. During the late summer and early autumn, rainfall is related to the intense convection over the interior Amazon basin that is associated with the South American summer monsoon (SASM)<sup>8</sup>. From December to March, a northwesterly low-level flow, the Andean low-level jet (ALLJ), transports Amazon tropical moisture from interior Brazil near the Equator towards the South Atlantic Convergence Zone (SACZ) located over southern Brazil<sup>9</sup>. At the study site (27° S), a significant fraction of summer precipitation derives from this moisture flux<sup>10</sup>.

Thus, although it is not directly beneath the centre of convective activity over the Amazon basin, summer rainfall in southeastern Brazil is strongly influenced by the southward progression of convection across the Amazon basin through the summer. The two sources of rainfall also have quite distinct oxygen isotopic ratios. The more locally sourced winter rainfall is enriched in <sup>18</sup>O compared to summer precipitation, with average  $\delta^{18}\text{O}$  values of precipitation during the winter of  $-3\text{‰}$  as compared to average values of  $-7\text{‰}$  in the early autumn at Porto Alegre City, southern Brazil<sup>11</sup> (and see Supplementary Information S2). At present the mean annual isotopic composition of rainfall is mainly determined by the relative contribution of summer, monsoonal precipitation versus winter, extratropical precipitation and not by temperature or amount effects. This interpretation is supported by the coincidence of more positive values of  $\delta^{18}\text{O}$  with the rainiest period in Porto Alegre during winter and early spring, which is contrary to the expected tendency if either temperature or precipitation amount were the major source of variation in rainfall oxygen isotope ratios<sup>12</sup>.

Stalagmite BT2 was collected from Botuverá Cave (27° 13′ 24″ S; 49° 09′ 20″ W, 230 m above sea level, a.s.l.). On the basis of 20 U/Th analyses, the 70-cm-long stalagmite was deposited from ~116 thousand years (kyr) ago to the present without detectable hiatuses (Fig. 1). Samples for stable isotopic analyses were taken every 1 mm, which represents an average resolution of ~150 yr. Values of  $\delta^{18}\text{O}$  for stalagmite BT2 range from  $-0.5$  to  $-5.0$  with an apparent cyclicity of ~20 kyr (Fig. 2). The lowest values are observed around 14–20 kyr ago and around 40–45 kyr ago. Superimposed on the longer-term cyclicity are more abrupt millennial-scale variations with an amplitude of ~1 to 1.5‰.

Stalagmite BT2 appears to have been deposited in approximate isotopic equilibrium with cave drip water as indicated by the relatively small ranges of  $\delta^{18}\text{O}$  along single speleothem (such as stalactites or stalagmites) layers<sup>13</sup> (S3a) and absence of significant correlations between  $\delta^{18}\text{O}$  and  $\delta^{13}\text{C}$  (Supplementary Information S3b and c). The relatively large range of variation in  $\delta^{18}\text{O}$ , more than 5‰ in the speleothem, also suggests that temperature, through its effect in the calcite–water fractionation factor, is not the primary cause of the observed variation. The temperature-dependent fractionation between calcite and water is  $-0.24\text{‰ per }^\circ\text{C}$  (ref. 14), requiring 20 °C of temperature change to explain the total range of variation in  $\delta^{18}\text{O}$ , or more than twice what is thought to be the total

temperature change between glacial and interglacial climates in the subtropics<sup>15,16</sup>. Furthermore, the colder temperatures of the glacial period at ~18 kyr ago would result in more positive calcite  $\delta^{18}\text{O}$  values, not more negative as is observed during the Last Glacial Maximum. We conclude that  $\delta^{18}\text{O}$  of speleothem BT2 primarily reflects changes in  $\delta^{18}\text{O}$  of regional precipitation.

Figure 2 shows a comparison of the BT2 isotopic time series with incoming solar radiation for the month of February at 30° S. Variation in the latter is dominated by changes in precession of the Earth's orbit<sup>17</sup>. For each of the last five precessional cycles, minima and maxima in solar radiation align remarkably well with maxima and minima, respectively (the scale for insolation in Fig. 2 is reversed), in calcite  $\delta^{18}\text{O}$ . In addition, amplitude of the isotopic variation matches that of insolation. Spectral analysis of the BT2 record shows a dominant peak in spectral power at 23 kyr (see Supplementary Information S4), as does precession. By far the majority of the variance in  $\delta^{18}\text{O}$  is related to changes in insolation. Insolation could affect the isotopic composition of precipitation, and stalagmite BT2, in two main ways.

First, on the basis of modern isotopic climatology, we interpret increases in the isotopic values to reflect a greater proportion of winter versus summer rainfall. This seasonal balance in precipitation is in turn controlled by the long-term mean location and southward extent of convective activity associated with the South American summer monsoon and southern boundary of the Hadley cell in the Southern Hemisphere. Because of its location, the isotopic record of stalagmite BT2 should also record changes in the location of the SACZ. Indeed, the SACZ is the exit region of the monsoon low-level winds and its intensity during summer reflects the moisture convergence associated with this monsoon flow<sup>18</sup>. During minima in summer solar radiation in the Southern Hemisphere tropics and subtropics, the mean location of the SASM and the SACZ may shift northward and less Amazon basin moisture will be captured and transported towards the southeast, decreasing the relative contribution of summer monsoonal rainfall. The opposite will be true when summer insolation is at a maximum.

Second, insolation could influence the isotopic composition of rainfall and stalagmite BT2 by affecting the intensity of convection

in both SASM and the SACZ. Convective intensity could affect the isotopic composition of rainfall through an amount effect. Speleothem  $\delta^{18}\text{O}$  values, particularly those from the tropics or subtropics<sup>5,6</sup>, are often interpreted as indicating changes in the amount of rainfall because rainfall amount and  $\delta^{18}\text{O}$  are observed to be inversely correlated in regions of deep convection<sup>19</sup>. Periods of increased summer insolation in the region should be periods of increased convection, increased precipitation and decreased  $\delta^{18}\text{O}$  values of that precipitation. In fact, today  $\delta^{18}\text{O}$  over southern Brazil (Porto Alegre) is significantly correlated with monsoon intensity and the southward extent of the SASM<sup>20</sup>. During periods of increased convection and precipitation associated with an intensified SASM, the remaining water vapour—which is subsequently transported towards the SACZ by the ALLJ—is more depleted in  $\delta^{18}\text{O}$ . An intensified SASM over tropical South America leads to enhanced tropical convection and preferential rainout of  $^{18}\text{O}$  over the Amazon and ultimately to more depleted  $\delta^{18}\text{O}$  downstream<sup>20</sup>. Thus, changes in convective intensity within the SASM/SACZ may significantly contribute to and reinforce the effect that the location of this system has on the  $\delta^{18}\text{O}$  of precipitation. The BT2 record probably reflects both of these processes and suggests that both effects are primarily steered by precession-driven changes in solar insolation. Maxima in solar insolation in Southern Hemisphere summer result in maximum movement of the SASM/SACZ to the south and intensified convective activity in this system.

A comparison of the Holocene portion of our record with other studies of climate change in South America supports this interpretation. The BT2 isotopic record becomes progressively more negative over the course of the Holocene, during which time palynological studies indicate expansion of the Atlantic rainforest in coastal regions of southern Brazil<sup>21</sup> and a southward expansion of the Amazon rainforest along its southwestern border<sup>22</sup>. Studies of lakes on the Peruvian and Bolivian Altiplano also indicate increasing available moisture, sourced from the Amazon basin, over the course of the Holocene<sup>23,24</sup>.

The  $\delta^{18}\text{O}$  values of stalagmite BT2 also show a strong correspondence with atmospheric methane concentrations (Fig. 2) as determined from ice-core records in Greenland<sup>25</sup>. Rapid increases in methane concentrations are coincident with rapid increases in  $\delta^{18}\text{O}$

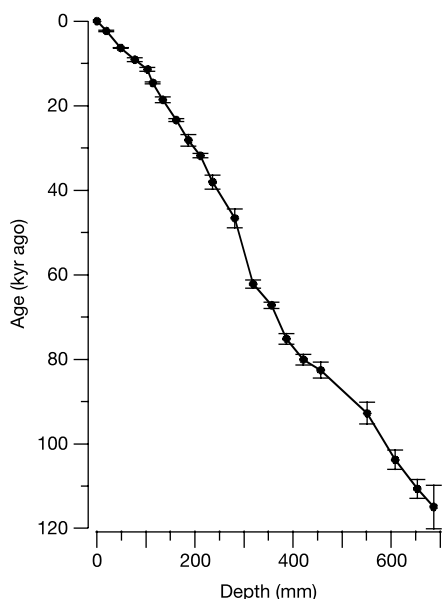


**Figure 1** Age versus depth model for stalagmite BT2. Error bars are 95% confidence limits. The solid line connecting the data points is the linear interpolation used to calculate ages of individual oxygen isotope data points.

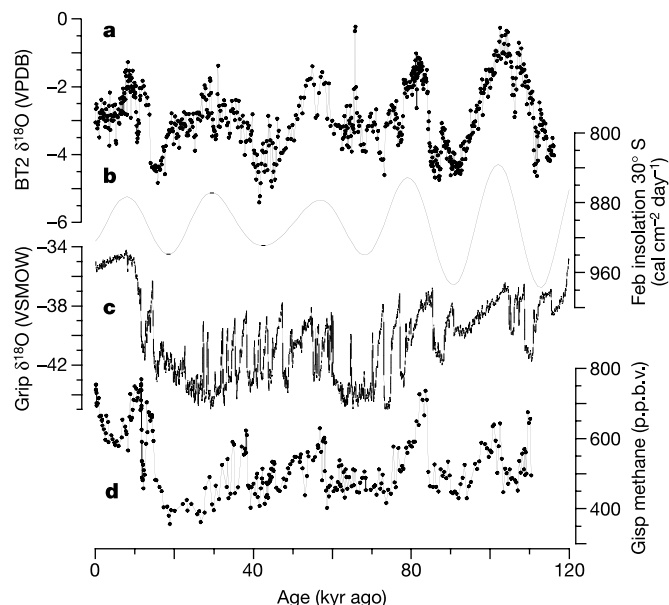


**Figure 2** Stable oxygen isotope profile for stalagmite BT2. The BT2 profile (a) is compared with February solar insolation for 30° S (b), oxygen isotopes of the NGrIP ice core from Greenland (c), and atmospheric methane concentrations from the Greenland ice core (d).

in our record and, if our interpretation is correct, with rapid northward shifts in the mean location of the South American monsoon. We suggest that during these periods the centre of convective activity related to the SASM was probably displaced northward, resulting in increased moisture and increased methane production in tropical wetlands. In addition to the movement of the monsoon a general intensification of the mean zonal Hadley circulation and tropical convective activity may have accompanied these shifts. This mechanism is also valid for the short-term negative trend in BT2 during the Younger Dryas period, which is consistent with rapid southward movement of the South American monsoon. During this time there is evidence of significant decrease in discharge of the Amazon River due to decreased monsoon precipitation in lowland tropical South America<sup>26</sup>.

Although precessional-scale changes in solar radiation appear to be the dominant driver of climate change in the region, other factors must also be involved. First, changes in the  $\delta^{18}\text{O}$  value of sea water also occurred and serve to dampen slightly the precession-driven changes. For example, seawater  $\delta^{18}\text{O}$  decreased by  $\sim 1\%$  during the transition from the Last Glacial Maximum to the Holocene<sup>27</sup>, during which time the BT2 isotopic values increased by  $\sim 3\%$ . Second, boundary conditions, in particular Northern Hemisphere ice volume and temperature, probably have an additional effect on the mean location of the South American monsoon that is superimposed on precession-driven changes even in the Southern Hemisphere. For example, the isotopic values of BT2 at  $\sim 17$  kyr ago and  $\sim 40$  kyr ago are about  $1.5\%$  more negative than at present, yet each of these three periods are close to maxima in solar radiation for Southern Hemisphere summers. Modelling studies indicate that during times of increased ice volume and decreased temperatures in the high northern latitudes, the intertropical convergence zone is pushed farther south than would be dictated by precession alone<sup>28</sup>. We suggest that the same is likely to be true for the SASM/SACZ system as a necessary response of the Hadley circulation in increasing its northward heat transport to compensate for the loss of energy caused by increased ice volume at high northern latitudes. In the study area, the result is an increase in the relative amount of monsoon-related precipitation in summer. Such a mechanism could explain, for example, the short, negative isotopic excursion in the BT2 record that occurs at the time of the Younger Dryas cold event in the Northern Hemisphere.

Figure 2 also compares the BT2  $\delta^{18}\text{O}$  values with isotopic data from the Grip Greenland ice core<sup>29</sup>. In the ice core, as in a variety of climate archives from the Northern Hemisphere from this time period, isotopic variation during the last glacial period is dominated by Dansgaard/Oeschger (D/O) cycles. In the BT2 time series, D/O-type cycles are observable as rapid  $1\text{--}2\%$  excursions in the isotopic values, although it is not possible to identify with certainty each individual D/O event in the BT2 record. The ages of more prominent, and more easily identifiable D/O events in the BT2 record match the absolute chronology of a speleothem record from Hulu Cave in China<sup>6</sup> quite well. In contrast to Northern Hemisphere records, however, in which D/O events are the primary mode of climate variation, the importance of D/O events is greatly reduced in our Southern Hemisphere record and precession-controlled changes in solar insolation dominate long-term variability in the tropical hydrological cycle. □

## Methods

Age determinations were carried out at Berkeley Geochronology Center, using conventional chemical and thermal ionization mass spectrometry (TIMS) techniques<sup>30</sup>. Twenty samples, weighting between 409 and 440 mg were cleaned ultrasonically in alcohol, totally dissolved by attack with concentrated  $\text{HNO}_3$  and equilibrated with a  $^{236}\text{U}\text{--}^{233}\text{U}\text{--}^{229}\text{Th}$  spike. U and Th were separated by ion exchange columns, loaded onto outgassed rhenium filaments, and measured on a VG-Sector 54 mass spectrometer equipped with a high abundance-sensitivity filter and Daly-ion counter. Measured isotope ratios were corrected for minor amounts of initial U and Th using  $^{232}\text{Th}$  as an index isotope and assuming a typical silicate composition for the contaminant; that is, activity

ratios of  $^{232}\text{Th}/^{238}\text{U} = 1.21 \pm 0.6$ ,  $^{230}\text{Th}/^{238}\text{U} = 1.0 \pm 0.1$ , and  $^{234}\text{U}/^{238}\text{U} = 1.0 \pm 0.1$ . U–Th isotopic data and ages are shown in Supplementary Table 1. Age errors are 95% confidence limits.

Oxygen isotope ratios are expressed in  $\delta$  notation, the per mil deviation from the Vienna Pee-Dee Belemnite standard. For example, for oxygen,  $\delta^{18}\text{O} = [((^{18}\text{O}/^{16}\text{O})_{\text{sample}} / (^{18}\text{O}/^{16}\text{O})_{\text{VPDB}}) - 1] \times 1,000$ . For each measurement, approximately 200  $\mu\text{g}$  of powder was drilled from the sample and analysed with an on-line, automated, carbonate preparation system linked to a Finnigan Delta XL ratio mass spectrometer at the University of Massachusetts. Reproducibility of standard materials is  $0.08\%$  for  $\delta^{18}\text{O}$ .

Received 16 August 2004; accepted 11 January 2005; doi:10.1038/nature03365.

- Dansgaard, W. *et al.* Evidence for general instability of past climate from a 250-kyr ice-core record. *Nature* **364**, 218–220 (1993).
- Peterson, L. C. *et al.* Rapid changes in the hydrologic cycle of the tropical Atlantic during the Last Glacial. *Science* **290**, 1947–1951 (2000).
- Schulz, H., von Rad, U. & Erlenkeuser, H. Correlation between Arabian Sea and Greenland climate oscillations of the past 110,000 years. *Nature* **393**, 54–57 (1998).
- Allen, J. R. M. *et al.* Rapid environmental changes in southern Europe during the last glacial period. *Nature* **400**, 740–743 (1999).
- Burns, S. J., Fleitmann, D., Kramers, J., Matter, A. & Al-Subbaray, A. Indian Ocean climate during the last glacial period and an absolute chronology for Dansgaard/Oeschger oscillations 9 to 13. *Science* **301**, 1365–1367 (2003).
- Wang, Y. J. *et al.* A high-resolution absolute-dated late Pleistocene monsoon record from Hulu Cave, China. *Science* **294**, 2345–2348 (2001).
- Vera, C. S., Vignarolo, P. K. & Berbery, E. H. Cold season synoptic-scale waves over subtropical South America. *Mon. Weath. Rev.* **130**, 684–699 (2002).
- Zhou, J. & Lau, K. M. Does a monsoon climate exist over South America? *J. Clim.* **11**, 1020–1040 (1998).
- Gan, M. A., Kousky, V. E. & Ropelewski, C. F. The South American monsoon circulation and its relationship to rainfall over West-Central Brazil. *J. Clim.* **17**, 47–66 (2004).
- Rao, V. B., Cavalcanti, I. F. A. & Hada, K. Annual variation of rainfall over Brazil and water vapor characteristics over South America. *J. Geophys. Res.* **101**, 26539–26551 (1996).
- IAEA/WMO. *Global Network for Isotopes in Precipitation (GNIP) Database* (IGBP PAGES/World Data Center-A for Paleoclimatology Data Contribution Series 94–005 NOAA/NGDC Paleoclimatology Program, Boulder, Colorado, 1994); (<http://isohis.iaea.org>).
- Rozanski, K., Araguás-Araguás, L. L. & Gonfiantini, R. In *Climate Change in Continental Isotopic Records* (eds Swart, P. K., Lohmann, K. C., McKenzie, J. & Savin, S.) 1–36 (Geophysical Monograph 78, American Geophysical Union, Washington, DC, 1993).
- Hendy, C. H. The isotopic geochemistry of speleothems. I. The calculation of the effects of different modes of formation on the isotopic composition of speleothems and their applicability as paleoclimatic indicators. *Geochim. Cosmochim. Acta* **35**, 801–824 (1971).
- Friedman, I. & O'Neil, J. R. In *Data of Geochemistry* (ed. Fleischer, E. M.) Ch. KK, 1–12 (United States Geological Survey Professional Paper 440-KK, US Government Printing Office, Washington, DC, 1977).
- Stute, M. *et al.* Cooling of tropical Brazil ( $5^\circ\text{C}$ ) during the last glacial maximum. *Science* **269**, 379–383 (1995).
- Lea, D., Pak, D. K., Peterson, L. C. & Hughen, K. A. Synchronicity of tropical and high latitude temperature over the last glacial termination. *Science* **301**, 1361–1364 (2003).
- Berger, A. & Loutre, M. F. Insolation values for the climate of the last 10 million years. *Quat. Sci. Rev.* **10**, 297–317 (1991).
- Nogués-Paegle, J. & Mo, K. C. Alternating wet and dry conditions over South America during summer. *Mon. Weath. Rev.* **125**, 279–291 (1997).
- Gat, J. R. Oxygen and hydrogen isotopes in the hydrologic cycle. *Annu. Rev. Earth Planet. Sci.* **24**, 225–262 (1996).
- Vuille, M., Bradley, R. S., Werner, M., Healy, R. & Keimig, F. Modeling  $\delta^{18}\text{O}$  in precipitation over the tropical Americas: 1. Interannual variability and climatic controls. *J. Geophys. Res.* **108**, 4174, doi:10.1029/2001JD002038 (2003).
- Behling, H. South and Southeast Brazilian grasslands during Late Quaternary times: a synthesis. *Palaeoogeogr. Palaeoecol. Palaeoecol.* **177**, 19–27 (2002).
- Mayle, F. E., Burbridge, R. & Killeen, T. J. Millennial-scale dynamics of southern Amazonian rain forests. *Science* **290**, 2291–2294 (2000).
- Baker, P. A. *et al.* The history of South American tropical precipitation for the past 25,000 years. *Science* **291**, 640–643 (2001).
- Seltzer, G., Rodbell, D. & Burns, S. J. Isotopic evidence for Late Glacial and Holocene hydrologic change in tropical South America. *Geology* **28**, 35–38 (2000).
- Brook, E. J., Sowers, T. & Orcharto, J. Rapid variations in atmospheric methane concentration during the past 110,000 years. *Science* **273**, 1087–1091 (1996).
- Maslin, M. A. & Burns, S. J. Reconstruction of the Amazon Basin effective moisture availability over the past 14,000 years. *Science* **290**, 2285–2287 (2000).
- Schrag, D. *et al.* The oxygen isotopic composition of seawater during the Last Glacial Maximum. *Quat. Sci. Rev.* **21**, 331–342 (2002).
- Chiang, J. C. H., Biasutti, M. & Battisti, D. S. Sensitivity of the Atlantic Intertropical Convergence Zone to the Last Glacial Maximum boundary conditions. *Paleoceanography* **18**(4), 1094, doi: 10.1029/2003PA000916 (2003).
- North Greenland Ice Core Project members. High resolution record of Northern Hemisphere climate extending into the last interglacial period. *Nature* **431**, 147–151 (2004).
- Sharp, W. D., Ludwig, K. R., Chadwick, O. A., Amundson, R. & Glaser, L. L. Dating fluvial terraces by  $^{230}\text{Th}/\text{U}$  on pedogenic carbonate, Wind River Basin, Wyoming. *Quat. Res.* **59**, 139–150 (2003).

Supplementary Information accompanies the paper on [www.nature.com/nature](http://www.nature.com/nature).

**Acknowledgements** We thank the Fundação de Amparo a Pesquisa do Estado de São Paulo (FAPESP) for financial support, the CECAV/IBAMA for authorizing cave samples collection and the GEEP-Açungui Speleological Group and E. Barni for supporting field work.

**Competing interests statement** The authors declare that they have no competing financial interests.

**Correspondence** and requests for materials should be addressed to F.W.C. Jr (fdacruz@geo.umass.edu).

## Water-rich basalts at mid-ocean-ridge cold spots

Marco Ligi<sup>1</sup>, Enrico Bonatti<sup>1,2,3</sup>, Anna Cipriani<sup>1,2</sup> & Luisa Ottolini<sup>4</sup>

<sup>1</sup>Istituto Scienze Marine, Geologia Marina, CNR, Via Gobetti 101, 40129 Bologna, Italy

<sup>2</sup>Lamont Doherty Earth Observatory, Columbia University, Palisades, New York 10964, USA

<sup>3</sup>Dipartimento di Scienze della Terra, Università “La Sapienza”, Piazzale Aldo Moro 5, 00187 Rome, Italy

<sup>4</sup>Istituto di Geoscienze e Georisorse, Sezione di Pavia, CNR, Via Ferrata 1, 27100 Pavia, Italy

Although water is only present in trace amounts in the sub-oceanic upper mantle, it is thought to play a significant role in affecting mantle viscosity, melting and the generation of crust at mid-ocean ridges. The concentration of water in oceanic basalts<sup>1,2</sup> has been observed to stay below 0.2 wt%, except for water-rich basalts sampled near hotspots and generated by ‘wet’ mantle plumes<sup>3–5</sup>. Here, however, we report unusually high water content in basaltic glasses from a cold region of the mid-ocean-ridge system in the equatorial Atlantic Ocean. These basalts are sodium-rich, having been generated by low degrees of melting of the mantle, and contain unusually high ratios of light versus heavy rare-earth elements, implying the presence of garnet in the melting region. We infer that water-rich basalts from such regions of thermal minima derive from low degrees of ‘wet’ melting greater than 60 km deep in the mantle, with minor

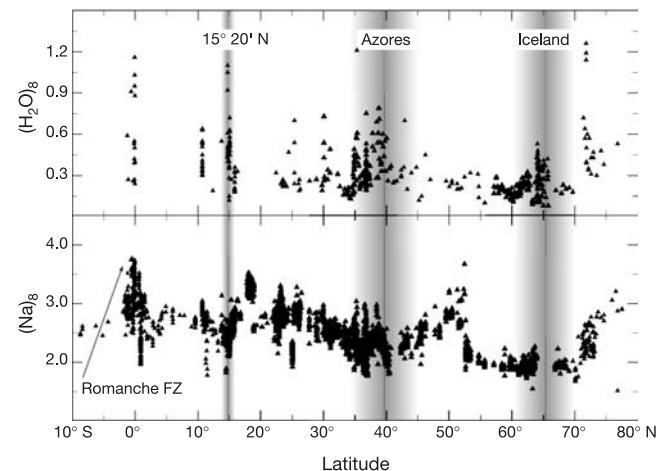


**Figure 1** Distribution of Na<sub>2</sub>O<sub>8</sub> and H<sub>2</sub>O<sub>8</sub> in MORB glasses along the axis of the Mid-Atlantic Ridge from Iceland to the Equator. Data are from the Supplementary Table, our unpublished results and the Petrological Database of the Ocean Floor (PETDB) of Lamont Doherty Earth Observatory. FZ, fracture zone.

dilution by melts produced by shallower ‘dry’ melting—a view supported by numerical modelling. We therefore conclude that oceanic basalts are water-rich not only near hotspots, but also at ‘cold spots’.

The water content of the oceanic upper mantle can be estimated from the water concentration in mid-ocean-ridge basalt (MORB) glasses, after correcting for the effects of degassing and magmatic differentiation. The H<sub>2</sub>O content of normal MORB (N-MORB) is generally below 0.2 wt% (ref. 1). Given that H<sub>2</sub>O is about as incompatible as Ce, and assuming ~10% average degree of melting of the mantle upwelling below mid-ocean ridges (MORs), the mantle source of N-MORB is assumed to contain 0.01–0.02 wt% H<sub>2</sub>O (ref. 2). However, basalts from topographically swollen portions of MORs have H<sub>2</sub>O concentrations higher than those of N-MORB (Fig. 1). These swollen ridges are generally interpreted as being influenced by hot plumes rising from the transition zone or from even deeper in the mantle. Thus, the H<sub>2</sub>O content of the mantle source of plume-type oceanic basalts is probably significantly higher than that of the N-MORB source region. For example, the mantle source of the Icelandic<sup>3</sup> and Azores platform<sup>4</sup> crust contains between 620 and 920 p.p.m. H<sub>2</sub>O, that is, several times higher than that of the N-MORB source. Concerning off-ridge hotspots, an H<sub>2</sub>O content of 405 ± 190 p.p.m. has been estimated for the mantle source of Hawaiian basalts<sup>5</sup>, supporting the hypothesis that plume-type mantle is H<sub>2</sub>O-rich relative to the N-MORB mantle source. High water and volatile contents lower the mantle solidus, so that the mantle melts deeper and to a higher degree during its ascent below MORs.

We report here that the H<sub>2</sub>O content of basaltic glasses from the equatorial Mid-Atlantic Ridge (MAR) is significantly higher than that of N-MORB. However, these H<sub>2</sub>O-rich basalts are associated not with a ‘hot’ portion of MOR, but with the opposite—that is, a thermal minimum in the ridge system. We will discuss a model that

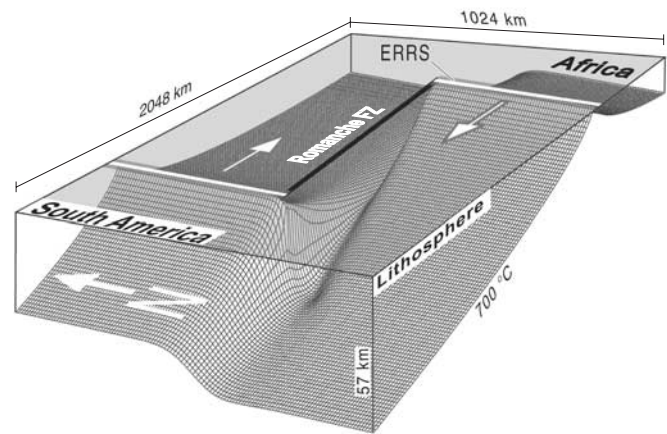


**Figure 2** Geometry of the passive-flow model. The bases of the rigid plates represent the upper boundary layer in our plate-thickening passive mantle flow model. The model shown was obtained by iteratively solving the mantle temperature field at each time step, starting from a constant-thickness plate-flow model. The computed thickness of the African plate lithosphere at the ERRS transform intersection is ~50 km. Mantle flow velocities were estimated by solving a steady-state corner flow in a computational frame 2,048 × 1,024 km wide and 150 km deep (using a grid with 2 × 2 km spacing for each 1 km depth increment), assuming an incompressible homogeneous and isoviscous mantle. Mantle temperatures were predicted by solving the steady-state advection-diffusion equation, using an over-relaxation upwind finite difference method with variable grid spacing (512 × 256 × 101), and highest grid resolution (1 km) at the plate boundaries<sup>28</sup>. Temperature solutions were found assuming 0 °C at the sea floor and 1,330 °C at 150 km depth, assuming the presence of an equatorial MAR cold spot<sup>11,12</sup>.